doi:10.2533/chimia.2017.295 Chimia 70 (2017) 295–298 © Swiss Chemical Society

Ultrafast Laser to Tailor Material Properties: An Enabling Tool in Advanced Three-dimensional Micromanufacturing

Yves Bellouard*

Abstract: The progress made in ultrafast laser technology towards high repetition rate systems have opened new opportunities in micromanufacturing. Non-linear absorption phenomena triggered by femtosecond pulses interacting with transparent materials allow material properties to be tailored locally and in three dimensions, with resolution beyond the diffraction limits and at rate compatible with fabrication process requirements. In this short article, we illustrate the potential of this technology for manufacturing, and more specifically micro-engineering, with a few examples taken from our own research and beyond.

Keywords: Micro-engineering · Ultrafast laser

Introduction: Femtosecond Laser Processing on Dielectrics

Tightly focused femtosecond laser pulses of ultrashort duration (10^{-13}–10^{-15} s) applied to transparent substrates trigger non-linear absorption phenomena such as multiphoton processes, ionizing the focal volume, creating a plasma that once recombining with the material structure lead to a locally modified structure. This laser–matter interaction, complex and diverse, differs from one material system to another.[1–8]

Among the various dielectric substrates, fused silica combines an ensemble of unique characteristics that make it, when exposed to femtosecond laser radiation, a particularly interesting candidate for multifunctional integration in monolithic substrates.

In these materials, one can locally increase the refractive index,[9,10] enhance the etching rate,[11] introduce sub-wavelength patterns[12] with associated form birefringence,[13,14] create voids[15] or change the thermal properties of fused silica.[16] By scanning the laser through the specimen volume,[17] one can distribute, combine and organize these material modifications to form complex patterns to be used for instance as waveguides or fluidic channels.

The basic working principle of the femtosecond laser direct-writing process is illustrated in Fig. 1.

Three-dimensional Micromachining

Using a two-step process that combines laser exposure and chemcial etching, complex parts with three-dimensional (3D) geometries can be efficiently produced. As will be seen later on, the chemical step has a beneficial effect on the mechanical properties of the fabricated microstructures by enhancing the surface quality and reducing the occurrence of possible micro-cracks. The steps toward micromachining of 3D parts are further described below and illustrated in Fig. 1:

Step 1: The material is selectively exposed by rasterizing a pattern according to a technique described in ref. [17]. As an illustration of the laser systems used in the examples presented in this paper, we used mainly ytterbium-based lasers operating around 1030 nm with typical pulse duration around 270-fs and repetition rates ranging from 400 to 800 kHz or above. Average power is typically in the range of a few to hundreds of milliwatts with pulse energies of a few tens of nano-Joules. Microscope objectives with moderate NA (typically around 0.4 to 0.6 NA) are often used. Writing speeds (that vary depending on the type of pattern) range from a few tens of microns per seconds to tens of mm per seconds. Higher writing speeds have been reported[18] and essentially depend

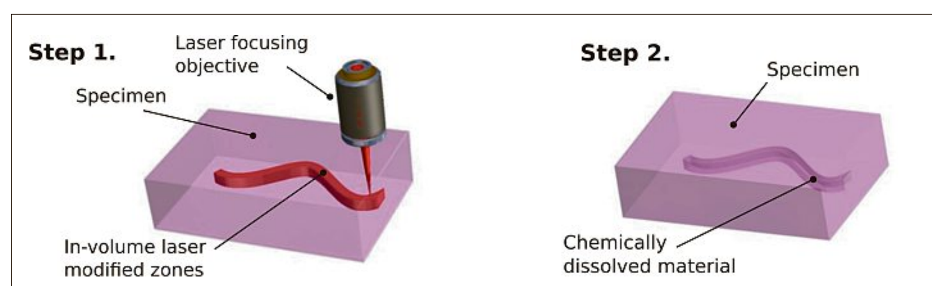

Fig. 1. Illustration of the processing steps for three-dimensional manufacturing using ultra-fast lasers,[17] illustrated here in the case of a micro-channel microfabrication. Step 1: The material is locally exposed to femtosecond laser irradiation, for instance, by locally moving the substrate under the laser beam or, by scanning the laser beam on a static substrate. The inner structure of the material is modified, but no ablation is taking place. As the process is non-linear, the laser light is locally absorbed only at the focal point. Modifications can therefore be three-dimensional and can occur anywhere within the volume of the glass and under the surface in particular. The nature of the structural changes induced by the laser can be diverse, ranging from continuously modified zones to self-organized patterns such as nanogratings. Furthermore, and as another consequence of the non-linearity of the interaction, the modified zone can be smaller than the spot-size itself and therefore, beyond the diffraction limit. Step 2: To remove material, the laser exposed region is etched away for instance with hydrofluoric (HF) acid in the case of silica. This second step is omitted when the laser modified zones are directly used for their properties (such as in the case of waveguides).

**Correspondence*: Prof. Dr. Y. Bellouard
EPFL STI/IMT, Galatea Lab
Rue de la Maladière 71b, CP526
CH-2002 Neuchâtel 2
E-mail: Yves.Bellouard@epfl.ch

on the strategy used to stir the beam or to move the specimen under it.

Step 2: After laser-exposure, the part is etched in a low-concentration hydrofluoric bath. Concentrations between 2.5% and 5% are typically used. With these concentrations, the etching rate enhancement is 60–120 times faster[17] in the exposed region compared to the pristine material. This may result in a total etching time that can vary from a few tens of minutes to several hours, depending on the complexity of the patterns. Noticeably, the laser polarization has a strong effect on the etching efficiency.[19] Recent work[20] has shown that KOH also provides an efficient and more selective means for structuring laser-exposed patterns with the aspect ratio exceeding thousand in certain cases. However, the etching mechanisms are different and lead to different surface morphologies. The two methods can eventually be combined, taking advantage of the characteristics of both.[21]

The mechanism leading to an etching rate enhancement is complex and not fully understood, but seems to be mainly driven by the localized densification and porosity introduced in the material as well as the presence of stress that is known to have an effect on the etching rate.[22]

Fig. 2 illustrates a monolithic three-dimensional flexure cross-pivot[23] entirely manufactured out of glass. Such flexures have superior performances compared to more traditional flexures like the notch hinge: the stiffness contrast between the pivot axis and the other degrees of freedom is significantly higher and better defined, making it a true one-degree of freedom pivot. As the figure shows, these cross-pivots can themselves be combined in more complex structures, *e.g.* mechanical guidance like the Hoecken mechanism illustrated below. This example illustrates how the process described above can be used to 'print' three-dimensional parts.

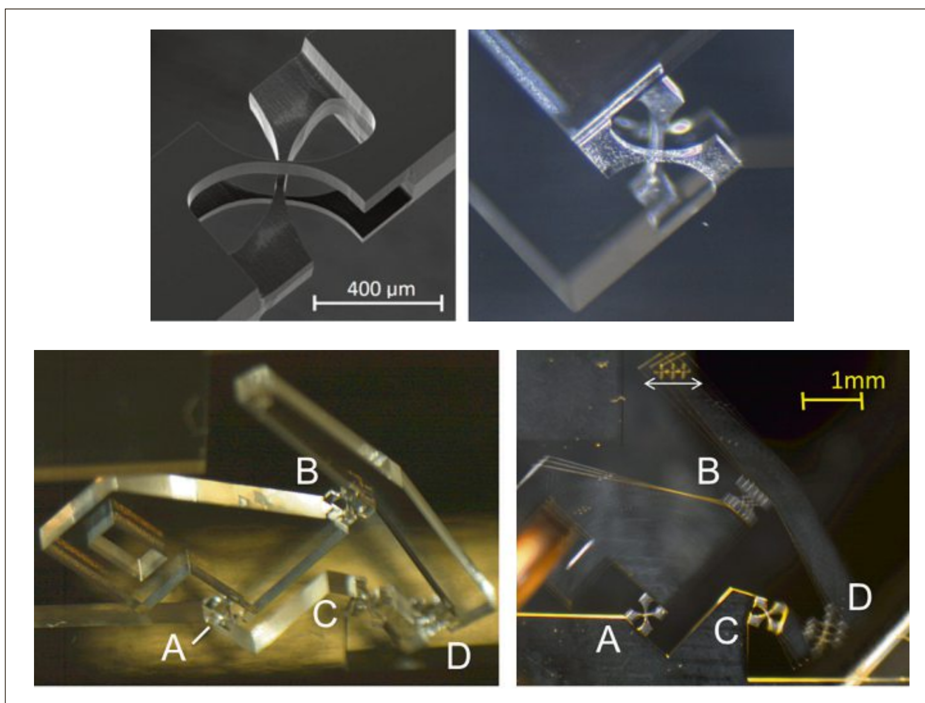

Fig. 2. Scanning Electron Microscope image (top left) and microscope image (top right) of a cross-pivot hinge as part of a mechanism. The images show the three crossed beams and the rounded corners at the location where the beams are connected to the main body. Note the high aspect ratio of the micromachining process. A monolithic glass Hoecken linear guidance (left) and a sequence of merged images to illustrate the function of the mechanism (right). The end point, *i.e.* where the linear motion is produced, is the cross in the upper part. The mechanism is activated by moving the rectangular window (left side of the images) along a circle. The linearity is within ±0.5 µm over a displacement of 600 µm. Figure taken from ref. [23].

Waveguide Writing

Waveguide writing has been one of the most studied applications of femtosecond laser processing of dielectrics and numerous examples can be found in the literature (a few references are provided for fused silica as well as other glass.[9,10,24–31] The topic has recently been reviewed in ref. [31]. The volume locally hit by the femtosecond laser experiences a slight increase of refractive index (highest reported Δn are in the order of ~0.5×10^{-3}). The laser affected zone (LAZ) shape and size can be determined using either a refractive index map technique or more recently a novel technique based on Scanning Thermal Imaging.[32] Losses in waveguides can be less than 0.4 dB/cm at 1550 nm, as reported by several authors. Complex optical devices can be formed by carefully combining waveguides splitting or separating them.[26,27,29]

Combining Laser-affected Zones of Different Kinds to Form Integrated Devices

An interesting aspect of this manufacturing technique is the fact that the same laser can produce more than one type of microstructure having different functions. In particular, waveguides and microstructures can be combined to form integrated devices such as optomechanical and optofluidics devices. As the same laser is used to produce all the features, such devices are intrinsically accurate as each element is produced at the same time.

Optofluidic Devices

To fabricate an optofluidic device, one needs to carefully control the etching process so that waveguides are preserved.[33,34] Using the technology platform introduced before, one can create a variety of small optofluidics instruments, for example where light propagating in waveguides is used to interrogate cells passing through a fluidic channel. The example below illustrates a fluidic microchip for identifying micro-algae[35,36] (illustrated in Fig. 3). The main advantage compared to other technology is that it is single monolith, optically transparent for a broad optical spectrum and compact.

Other examples of devices combining waveguides and channels can be found for instance in refs [37,38].

Micromechanics

Femtosecond lasers provide a way to carve out any shape from a glass material as long as the acid can penetrate through the laser exposed regions. One can therefore make fluidic structures as described above, but also flexures – a deformable element used in precision mechanics, by defining thin-beam-like structures that can deform elastically. Based on this principle, all-optical mechanical sensor[39] where the flexures and the waveguides are all part of the same material can be made. There, the structure withstands stress in excess of 500 MPa. Stress in excess of 2 GPa can even be reached in a single flexure.[40,41] The mechanical performance is strongly affected by the etching rate.

Controlled Stress State

The femtosecond laser–matter interaction in the non-ablative regime induces lo-

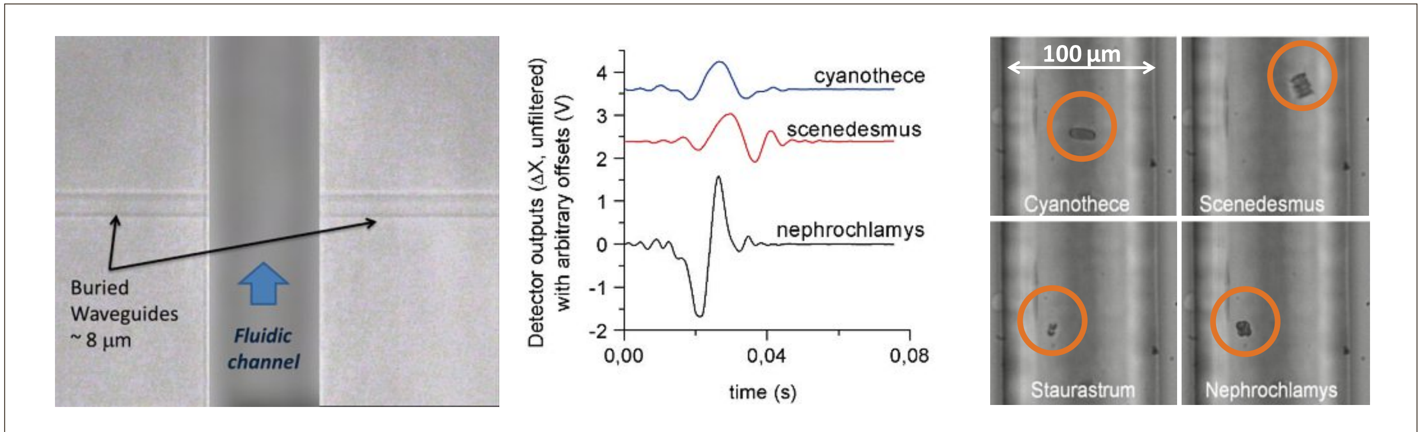

Fig. 3. Left: Channel and waveguides written in the bulk of glass (adapted from ref. [34], © SPIE). Center: Examples of wavelets signals obtained for specific algae species. Right: Images captured on the fly by a microscope camera overlooking the fluidic channel (center and right images taken from ref. [35], © Optical Society of America).

calized volume changes in the material. As a consequence, these density changes generate stress in the material that can be controlled both in intensity and direction.[42] By carefully arranging these stressed zones, one can create wave plates[43] or use it for deforming the material locally like for instance for adjusting the position of an element.[44]

Micro-actuators and Optomechanical Sensors

The same process can also be used for manufacturing devices like micro-actuators. An illustration of a comb-array linear actuator is illustrated in Fig. 4.[45] Here, the high-aspect ratio of the micromachining technique is used to achieve large actuation forces by creating a difference of electrical potential between parallel plates arranged in a comb. The gap being shorter on one side than on the other, a net force pulling the structure in one direction is generated. The pull-back force is provided by the stored elastic energy in the guiding elements. This define is completely transparent to light. The electrodes consist of an indium-tin-oxide simply deposited on the material.

Thanks to the three-dimensional capabilities of micro-manufacturing process, new types of actuating principles that could not be easily implemented at the microscale are studied. Illustrations are for instance dielectrophoretic actuators[46] that benefit from a three-dimensional electrode design that is able to generate a electrostatic field gradient.

The Structure of Laser-affected Zones in Silica

The structural changes causing the change of properties, like the increased refractive index or the localized enhanced etching rate have been analyzed using multiple spectroscopy techniques (see for instance refs [26,47–50] including Raman[51] as well as with indirect methods.[52,53] So far, it is generally admitted that two main types of modifications are found. Starting from the lowest to the highest pulse energies and for pulse energies below ~200 fs,[54] the first type of modification (Regime I) corresponds to a localized densification. This laser-induced densification mechanism appears to be different than densification induced by mechanical means as indicated by Raman observations.[32] While common features are observed such as the narrowing and shift of the main band, femtosecond laser-induced densification is characterized by an increase of the D2-peak amplitude, suggesting the formation of silica tetrahedral rings of lower order.

At higher pulse energy levels, one observes intriguing self-organization phenomena consisting of nanoplanes forming parallel one to another,[12] the so-called Regime II. Contrary to the lower pulse energy regime, these nanostructures, due to their periodicity, induce phenomena of form birefringence (*i.e.* a periodic modulation of the refractive index[13,14]) that is also characterized by a localized increase of volume. As shown in ref. [55], these nanoplanes contain porous materials into which the presence of molecular oxygen

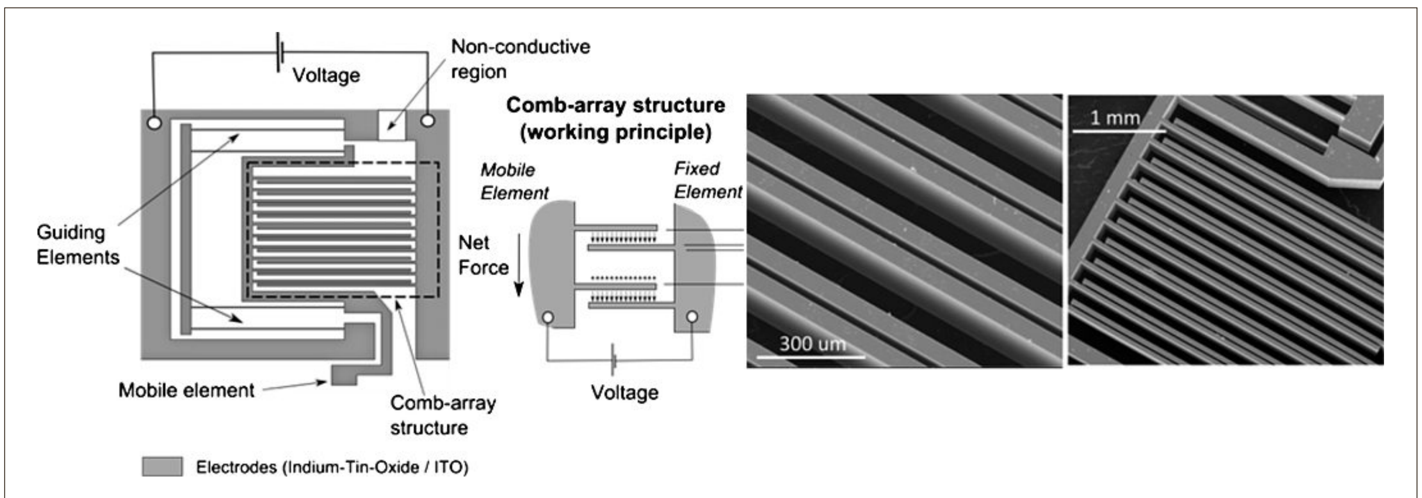

Fig. 4. Left: Working principle for a comb-array electrostatic glass actuator. Right: Scanning electron microscope close-up views of the fabricated comb-array actuator (adapted from ref. [45], © American Institute of Physics).

has been hypothesized[56] and recently experimentally confirmed.[57] The exact formation mechanism of these nanostructures is still actively debated and various models have been proposed (see among others refs [12,58–60]).

Interestingly, the pulse duration triggers or suppresses the occurrence of Regime I. Above 200 fs, this regime seems not to be observed,[54] at least using classical focusing techniques. The evolution of these laser-modified zones and their behavior strongly depends on the energy deposited in the material (also called net fluence or dose). For instance, one can observe a change from a volume reduction to an expansion of the laser-affected zone while continuously increasing the pulse energy of the laser, from regime I to regime II.[57] Noteworthy, this transition from shrinkage to expansion is also observed while continuously increasing the exposure dose in regime I.[57]

If the repetition rate of the laser is driven to a high level (typically above ~2–3 MHz for silica), one observes the bulk heating of the material[61,62] and the formation in particular of gas bubbles that may themselves self-organize by feedback mechanisms.[63]

Here, we have briefly surveyed some of the more well-known effects. Much remains to be done to fully understand this peculiar laser–matter interaction and to explore all its subtleties, but also to optimize it.

Conclusion and Future Prospects

Femtosecond lasers can be used to efficiently tailor the material properties of fused silica in order to create not only optical functions (such as waveguides), but also mechanical (flexures) or fluidic (microchannels) elements. These functions can be combined to form complex optofluidics or optomechanical devices or a combination of both in a single substrate of material. This dramatically reduces the fabrication complexity and opens new horizons for further integration at the micro-/nanoscale, in particular by offering the possibility to fabricate three-dimensional devices, which is difficult using conventional fabrication methods based on lithographic techniques.

The next step is to expand the taxonomy of functions that can be directly written in the material. To do so, one could imagine using femtosecond lasers to induce high-pressure polymorphic phases of the same material. For instance, in the case of SiO_2, there are numerous existing polymorphic phases, stable at ambient temperature, that have physical properties different from their amorphous counterpart. Well-known examples are the quartz phases that exhibit piezoelectricity while amorphous silica does not.

Acknowledgements

Part of this publication has been previously reported in Y. Bellouard, *SPIE Proceedings* **2015**, *9351*, 93510G, DOI: 10.1117/12.2086709.[64]

Received: April 26, 2017

[1] D. Du, X. Liu, G. Korn, J. Squier, G. Mourou, *Appl. Phys. Lett.* **1994**, *64*, 3071.
[2] B. C. Stuart, M. D. Feit, A. M. Rubenchik, B. W. Shore, M. D. Perry, *Phys. Rev. Lett.* **1995**, *74*, 2248.
[3] M. D. Perry, B. C. Stuart, P. S. Banks, M. D. Feit, V. Yanovsky, A. M. Rubenchik, *J. Appl. Phys*. **1999**, *85*, 6803.
[4] A.-C. Tien, S. Backus, H. Kapteyn, M. Murnane, G. Mourou, *Phys. Rev. Lett.* **1999**, *82*, 3883.
[5] S. S. Mao, F. Quéré, S. Guizard, X. Mao, R. E. Russo, G. Petite, P. Martin, *Appl. Phys. A: Mater. Sci. Proc.* **2004**, *79*, 1695.
[6] J. B. Ashcom, R. R. Gattass, C. B. Schaffer, E. Mazur, *JOSA B* **2006**, *23*, 2317.
[7] R. R. Gattass, E. Mazur, *Nat. Photon*. **2008**, *2*, 219.
[8] M. Beresna, M. Gecevičius, P. G. Kazansky, *Adv. Opt. Photon*. **2014**, *6*, 293.
[9] K. M. Davis, K. Miura, N. Sugimoto, K. Hirao, *Opt. Lett.* **1996**, *21*, 1729.
[10] K. Miura, J. Qiu, H. Inouye, T. Mitsuyu, K. Hirao, *Appl. Phys. Lett.* **1997**, *71*, 3329.
[11] A. Marcinkevicius, S. Juodkazis, M. Watanabe, M. Miwa, S. Matsuo, H. Misawa, J. Nishii, *Opt. Lett*. **2001**, *26*, 277.
[12] Y. Shimotsuma, P. G. Kazansky, J. Qiu, K. Hirao, *Phys. Rev. Lett.* **2003**, *91*, 247405.
[13] E. Bricchi, J. D. Mills, P. G. Kazansky, B. G. Klappauf, J. J. Baumberg, *Opt. Lett*. **2002**, *27*, 2200.
[14] E. Bricchi, B. G. Klappauf, P. G. Kazansky, *Opt. Lett.* **2004**, *29*, 119.
[15] E. N. Glezer, M. Milosavljevic, L. Huang, R. J. Finlay, T.-H. Her, J. P. Callan, E. Mazur, *Opt. Lett.* **1996**, *21*, 2023.
[16] Y. Bellouard, M. Dugan, A. A. Said, P. Bado, *Appl. Phys. Lett.* **2006**, *89*, 161911.
[17] Y. Bellouard, A. Said, M. Dugan, P. Bado, *Opt. Express* **2004**, *12*, 2120.
[18] M. Hermans, *J. Laser Micro/Nanoeng.* **2014**, *9*, 126.
[19] C. Hnatovsky, R. S. Taylor, E. Simova, V. R. Bhardwaj, D. M. Rayner, P. B. Corkum, *Opt. Lett.* **2005**, *30*, 1867.
[20] S. Kiyama, S. Matsuo, S. Hashimoto, Y. Morihira, *J. Phys. Chem. C* **2009**, *113*, 11560.
[21] S. LoTurco, R. Osellame, R. Ramponi, K. C. Vishnubhatla, *J. Micromech. Microeng.* **2013**, *23*, 085002.
[22] A. Agarwal, M. Tomozawa, *J. Non-Cryst. Solids* **1997**, *209*, 166.
[23] V. Tielen, Y. Bellouard, *Micromachines* **2014**, *5*, 697.
[24] Y. Sikorski, A. A. Said, P. Bado, R. Maynard, C. Florea, K. A. Winick, *Electron. Lett.* **2000**, *36*, 226.
[25] C. B. Schaffer, A. Brodeur, J. F. García, E. Mazur, *Opt. Lett.* **2001**, *26*, 93.
[26] A. M. Streltsov, N. F. Borrelli, *Opt. Lett.* **2001**, *26*, 42.
[27] K. Minoshima, A. M. Kowalevicz, I. Hartl, E. P. Ippen, J. G. Fujimoto, *Opt. Lett.* **2001**, *26*, 1516.
[28] R. Osellame, S. Taccheo, G. Cerullo, M. Marangoni, D. Polli, R. Ramponi, P. Laporta, S. De Silvestri, *Electron. Lett.* **2002**, *38*, 964.
[29] R. R. Thomson, S. Campbell, I. J. Blewett, A. K. Kar, D. T. Reid, S. Shen, A. Jha, *Appl. Phys. Lett*. **2005**, *87*, 121102.
[30] P. Bado, A. A. Said, M. Dugan, T. Sosnowski, in 'NFOEC', Vol. 2, Dallas (TX), **2002**, pp. 1153.
[31] T. Meany, M. Gräfe, R. Heilmann, A. Perez-Leija, S. Gross, M. J. Steel, M. J. Withford, A. Szameit, *Laser Photon. Rev*. **2015**, *9*, 363.
[32] Y. Bellouard, E. Barthel, A. A. Said, M. Dugan, P. Bado, *Opt. Express* **2008**, *16*, 19520.
[33] Y. Bellouard, A. Said, M. Dugan, P. Bado, in 'Materials Research Society Symposium - Proceedings', **2003**, *Vol. 782*, pp. 63.
[34] A. A. Said, M. Dugan, P. Bado, Y. Bellouard, A. Scott, J. R. Mabesa Jr., in 'Proceedings of SPIE - The International Society for Optical Engineering', **2004**, *Vol. 5339*, pp. 194.
[35] A. Schaap, Y. Bellouard, T. Rohrlack, *Biomed. Opt. Express* **2011**, *2*, 658.
[36] A. Schaap, T. Rohrlack, Y. Bellouard, *J. Biophoton.* **2012**, *5*, 661.
[37] R. W. J. Applegate, J. Squier, T. Vestad, J. Oakey, D. W. M. Marr, P. Bado, M. A. Dugan, A. A. Said, *Lab Chip* **2006**, *6*, 422.
[38] R. M. Vazquez, R. Osellame, D. Nolli, C. Dongre, H. van den Vlekkert, R. Ramponi, M. Pollnau, G. Cerullo, *Lab Chip* **2009**, *9*, 91.
[39] Y. Bellouard, A. Said, P. Bado, *Opt. Express* **2005**, *13*, 6635.
[40] Y. Bellouard, *Opt. Mater. Express* **2011**, *1*, 816.
[41] A. Champion, M. Beresna, P. Kazansky, Y. Bellouard, *Opt. Express* **2013**, *21*, 24942.
[42] C.-E. Athanasiou, Y. Bellouard, *Micromachines* **2015**, *6*, 1365.
[43] B. McMillen, C. Athanasiou, Y. Bellouard, *Opt. Express* **2016**, *24*, 27239.
[44] Y. Bellouard, *Opt. Express* **2015**, *23*, 29258.
[45] B. Lenssen, Y. Bellouard, *Appl. Phys. Lett.* **2012**, *101*, 103503.
[46] T. Yang, Y. Bellouard, *J. Micromech. Microeng.* **2015**, *25*, 105009.
[47] K. Hirao, K. Miura, *J. Non-Crystal. Solids* **1998**, *239*, 91.
[48] L. Skuja, *J. Non-Crystal. Solids* **1998**, *239*, 16.
[49] H.-B. Sun, S. Juodkazis, M. Watanabe, S. Matsuo, H. Misawa, J. Nishii, *J. Phys. Chem. B* **2000**, *104*, 3450.
[50] A. Zoubir, C. Rivero, R. Grodsky, K. Richardson, M. Richardson, T. Cardinal, M. Couzi, *Phys. Rev. B* **2006**, 73, 224117.
[51] J. W. Chan, T. Huser, S. Risbud, D. M. Krol, *Opt. Lett.* **2001**, *26*, 1726.
[52] Y. Bellouard, T. Colomb, C. Depeursinge, M. Dugan, A. A. Said, P. Bado, *Opt. Express* **2006**, *14*, 8360.
[53] A. Champion, Y. Bellouard, *Opt. Mater. Express* **2012**, *2*, 789.
[54] C. Hnatovsky, R. S. Taylor, P. P. Rajeev, E. Simova, V. R. Bhardwaj, D. M. Rayner, P. B. Corkum, *Appl. Phys. Lett.* **2005**, *87*, 014104.
[55] J. Canning, M. Lancry, K. Cook, A. Weickman, F. Brisset, B. Poumellec, *Opt. Mater. Express* **2011**, *1*, 998.
[56] M. Lancry, B. Poumellec, J. Canning, K. Cook, J.-C. Poulin, F. Brisset, *Laser Photon. Rev.* **2013**, *7*, 953.
[57] Y. Bellouard, A. Champion, B. McMillen, S. Mukherjee, R. R. Thomson, C. Pépin, P. Gillet, Y. Cheng, *Optica* **2016**, *3*, 1285.
[58] V. R. Bhardwaj, E. Simova, P. P. Rajeev, C. Hnatovsky, R. S. Taylor, D. M. Rayner, P. B. Corkum, *Phys. Rev. Lett.* **2006**, *96*, 057404.
[59] Y. Liao, J. Ni, L. Qiao, M. Huang, Y. Bellouard, K. Sugioka, Y. Cheng, *Optica* **2015**, *2*, 329.
[60] A. Rudenko, J.-P. Colombier, T. E. Itina, *Phys. Rev. B* **2016**, *93*, 075427.
[61] C. B. Schaffer, J. F. García, E. Mazur, *Appl. Phys. A: Mater. Sci. Proc.* **2003**, *76*, 351.
[62] S. Eaton, H. Zhang, P. Herman, F. Yoshino, L. Shah, J. Bovatsek, A. Arai, *Opt. Express* **2005**, *13*, 4708.
[63] Y. Bellouard, M.-O. Hongler, *Opt. Express* **2011**, *19*, 6807.
[64] Y. Bellouard, *SPIE Proceedings* **2015**, *9351*, 93510G, DOI: 10.1117/12.2086709.